J. Mol. Model. **2000**, *6*, 379 – 395

Journal of Molecular Modeling

FULL PAPER

Molecular Modeling of Fullerene Dendrimers

Hubert Schönberger[1], Christof H. Schwab[2], Andreas Hirsch[1], and Johann Gasteiger[2]

[1]Institut für Organische Chemie, Universität Erlangen-Nürnberg, Henkestr. 31, D-91054 Erlangen, Germany. {hubert.schoenberger, andreas.hirsch}@organik.uni-erlangen.de

[2]Computer-Chemie-Centrum, Institut für Organische Chemie, Universität Erlangen-Nürnberg, Nägelsbachstr. 25, D-91052 Erlangen, Germany. {christof.schwab, johann.gasteiger}@ccc.chemie.uni-erlangen.de

Received: 27 January 2000/ Accepted: 1 February 2000/ Published: 31 März 2000

Abstract The fullerene skeleton offers the possibility of attaching several dendrimer branches. Thus, starburst-dendrimers are obtained that might lead to self-limiting generation because of very large, sterically overburdened molecular systems. Two approaches for the generation of molecular models of such fullerene dendrimers are presented: Molecular mechanics and molecular dynamics calculations have been performed to explore the geometries and energetics of the compounds. The other approach utilized an empirical 3D structure generator that started from information on only the constitution of the molecules concerned.

Keywords Molecular dynamics, 3D model builder, CORINA, Self-limiting generation

Introduction

Dendritic molecules have been known for more than 20 years.[1] They feature a highly ordered shape and a cascade-like repetition of certain building blocks.[2,3] Among dendrimers, so-called "starburst-dendrimers", space-filling molecules bearing certain end-groups, are a subject of special interest.[4]

Dendrimers consisting of an initiator core of multiplicity Y and branches of multiplicity Z lead to $Y \bullet (Z)^X$ terminal groups in the Xth generation (Figure 1). As the diameter of a dendrimer grows linearly with the number of repetition steps while the volume of the functional groups in the outer sphere grows exponentially, a "self-limiting generation" may appear.[5] This generation is determined by Y and Z as well as by the dimensions of the building blocks, e.g. by the use of spacers.

The highest multiplicity attained so far for a symmetrical three-dimensional initiator core is Y = 4 for adamantane [6] and pentaerythrol [4] (Figure 2).

If the dendrimer synthesis is carried out in the presence of other molecules, these molecules can be incorporated into the dendritic structure. This is then called a "dendritic box". [7] Cavities and clefts within the dendritic structure can be utilized for the insertion of functional groups or to form host-guest-complexes with other molecules.

Topic of investigation

The intention of this investigation was to develop methods for the modeling of a new class of dendrimers synthesized

---

Correspondence to: A. Hirsch and J. Gasteiger

Dedicated to Professor Paul von Ragué Schleyer on the occasion of his 70th birthday

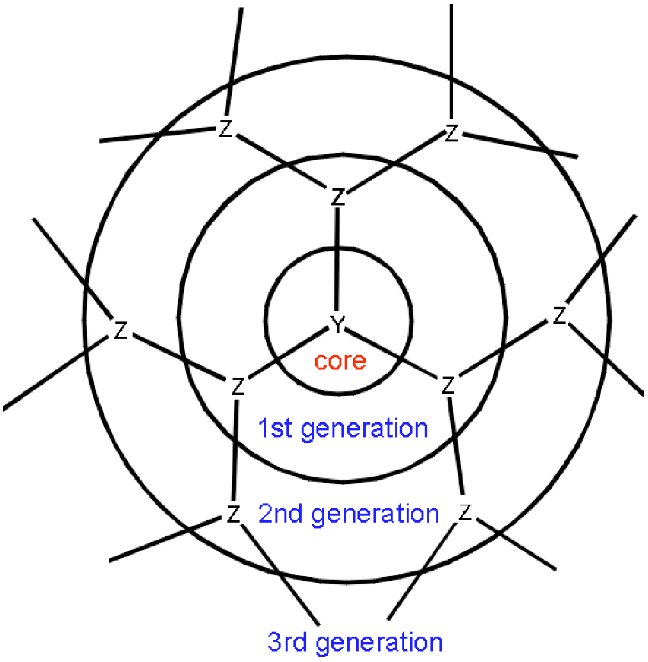

Figure 1 *Principle of dendritic growth*

for the first time by Hirsch *et al.*.[8] This new class of compounds exhibits an exceptionally high multiplicity of Y = 12 for the initiator core, the fullerene C_{60}, as shown in Figure 3. Fréchet-type benzyl ether dendrimers of a multiplicity of Z = 2 with rather short repetition units have been used as branches (Figure 4, see also [9]).

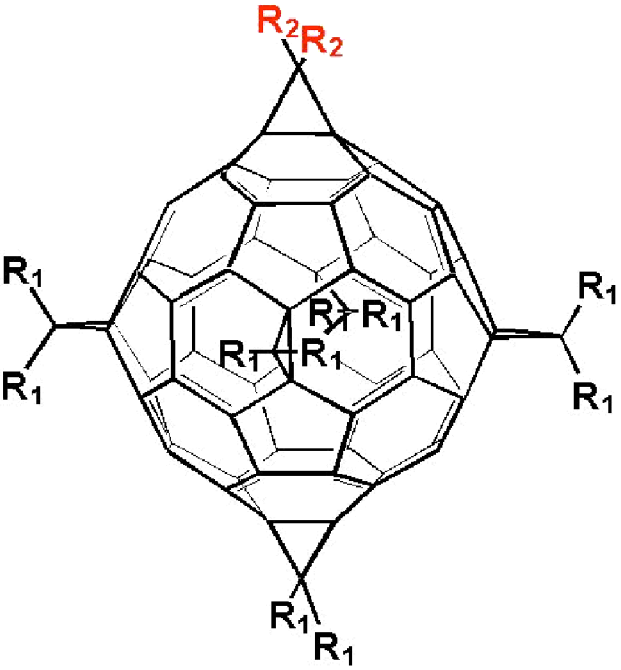

Figure 3 C_{60} *hexa-adduct leading to an initiator core with a multiplicity of Y = 12*

Figure 2 *Adamantane (left) and pentaerythrol (right): Up to now the highest known 3D multiplicity, Y = 4, of an initiator core*

Thus, only a small number of generations of the dendrimer should be necessary to reach sterically overburdened, compact structures.

Classical molecular mechanics and molecular dynamics calculations were carried out with the MM+ force field im-

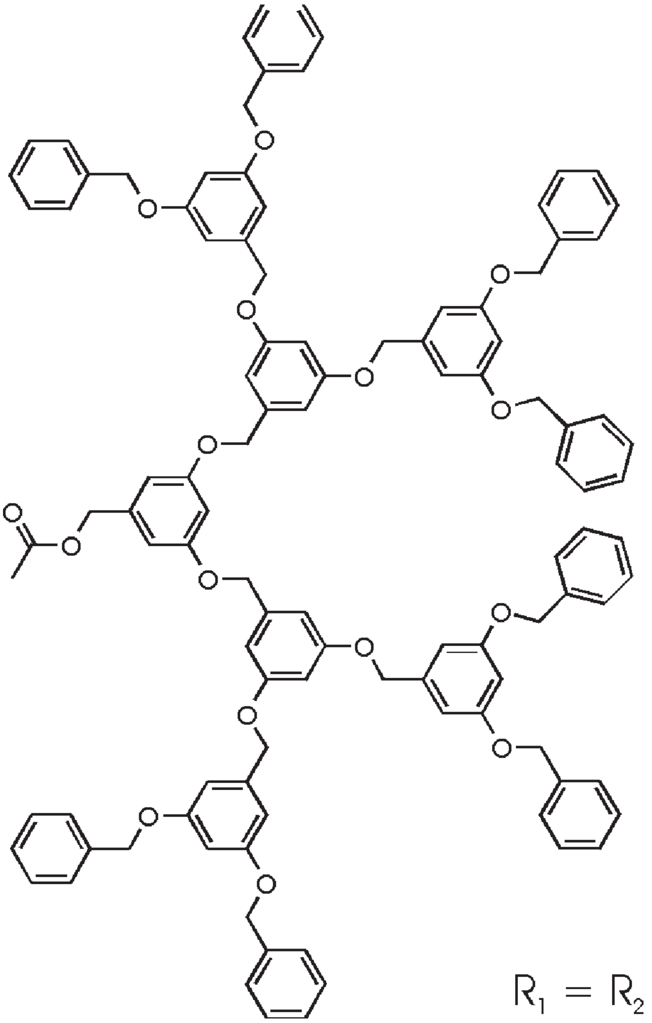

Figure 4 *Fréchet-type benzyl ether branches leading to a multiplicity of Z = 2*

Figure 5 *Cleft within a fullerene dendrimer to encapsulate guest molecules*

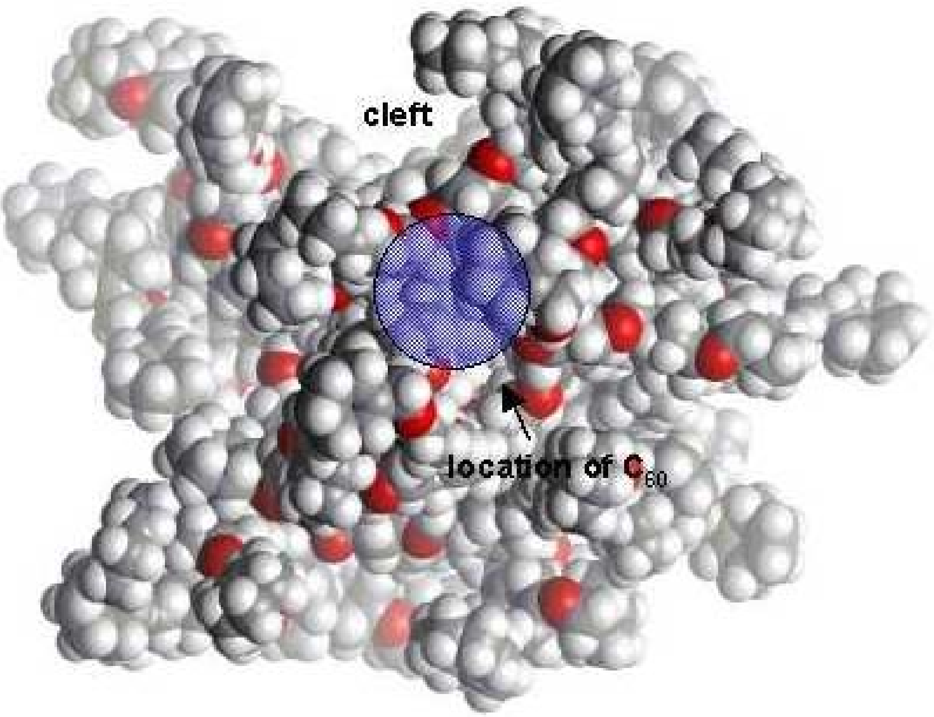

plemented in the software package HyperChem 4.5.[10] These geometries were compared to those obtained by the structure generation program CORINA.[11]

Based on these model systems (Figure 3) with R_1 and R_2, and $R_1 = R_2$, respectively, we intended to predict the structures of hexa-adducts in terms of availability of space in consecutive generations of the dendrimers.

As mentioned above, the fullerene dendrimers can form several clefts and cavities within the molecule. Figure 5 illustrates such a cleft in a fullerene dendrimer. Thus, an ad-

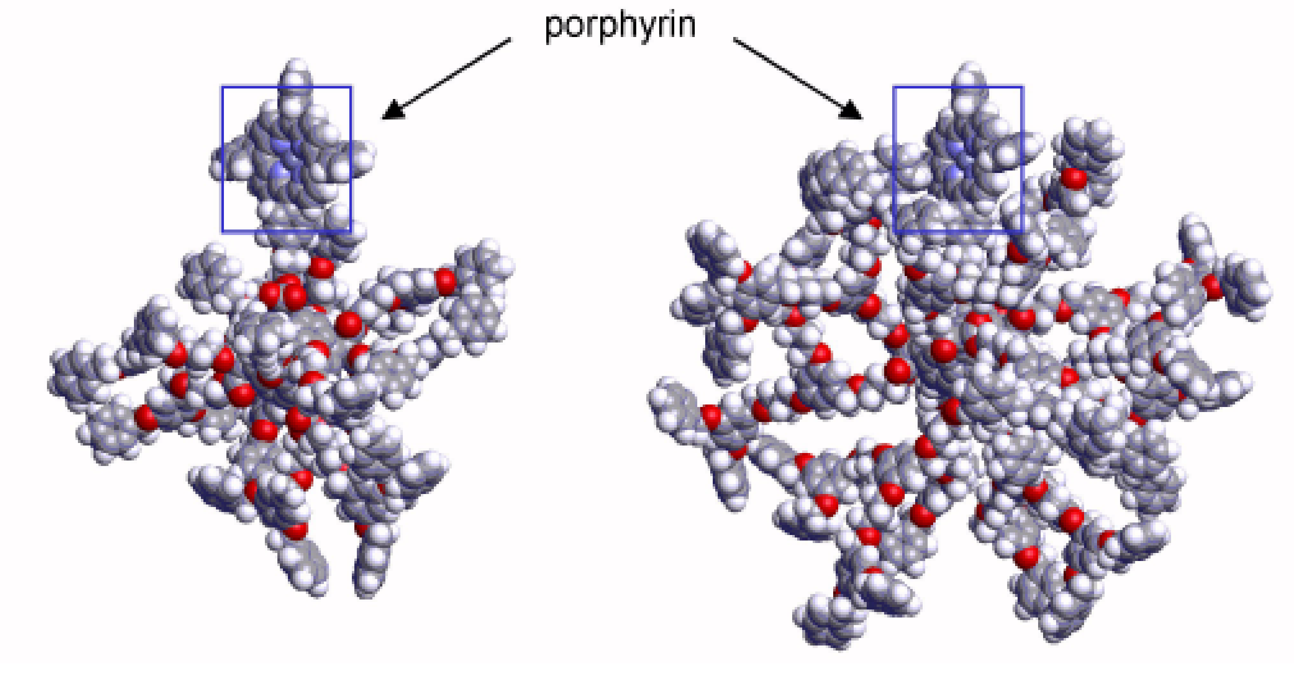

Figure 6 *Two different generations of fullerene dendrimers with porphyrins as functional groups*

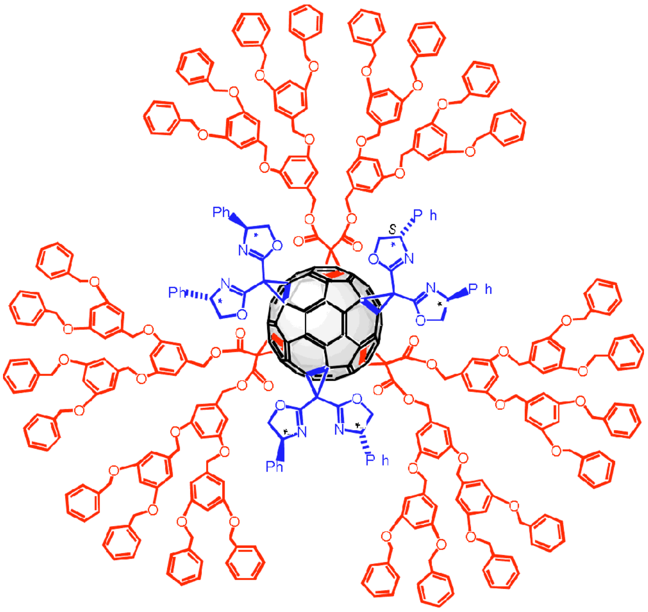

Figure 7 *Artificial enzyme ("chemzyme") promoting enantioselective cyclopropanation by synergism at the bisoxazoline units with the inherent chiral addition pattern of the fullerene*

duct of a fullerene core and a functional group exhibiting special chemical or electronic properties might leave enough empty space within the molecule after adding the dendritic branches to form host-guest-complexes with other molecules that are small enough to fit into the clefts and cavities.

Figure 6 shows two fullerene cores functionalized with porphyrin groups and two different generations of dendrimer branches. Interactions between the porphyrin groups and the fullerene cores strongly influence the electronic behavior of these compounds, so called dendrimer-encapsulated porphyrin fullerene diads.[12]

Furthermore, these functionalized fullerenes lead to the concept of "chemzymes",[13] artificial enzymes consisting of inherently chiral mixed hexa-adducts functionalized with catalytically active sites. Figure 7 gives an example for a "chemzyme".

With our comparative calculations we wished to gain information about the gas phase structure at ambient temperature and about possible solid-state structures. Finally, we tried to find evidence for the occurrence of a "self-limiting generation", which should result in strongly increasing energies due to close atom contacts within the molecule.

Methods

The packages for the molecular mechanics, molecular dynamics, and semiempirical quantum mechanical calculations are standard commercial software and are therefore only briefly mentioned. The software CORINA for the empirical construction of 3D molecular models is also a widely distributed commercial package. However, as it was developed in one of our research groups we are in a position to give more information on the scientific background of the methods contained in this software.

Molecular mechanics and molecular dynamics studies

Molecular mechanics calculations were performed with the MM+ force field implemented in the software package HyperChem 4.5. Molecular dynamics calculations were also carried out with the methods contained in HyperChem 4.5.

Semiempirical quantum mechanical calculations

The calculation of the structure and the molecular orbitals of the mono-adduct **7** was performed with AM1 contained in the software package SPARTAN.[14]

3D structure generator CORINA

The development of CORINA was initiated in 1984 and has matured through a series of versions ✳ [15-18]. It was originally developed to model the influence of the spatial arrangement of the atoms of a molecule on its reactivity within the reaction prediction program EROS,[19,20] but has found a

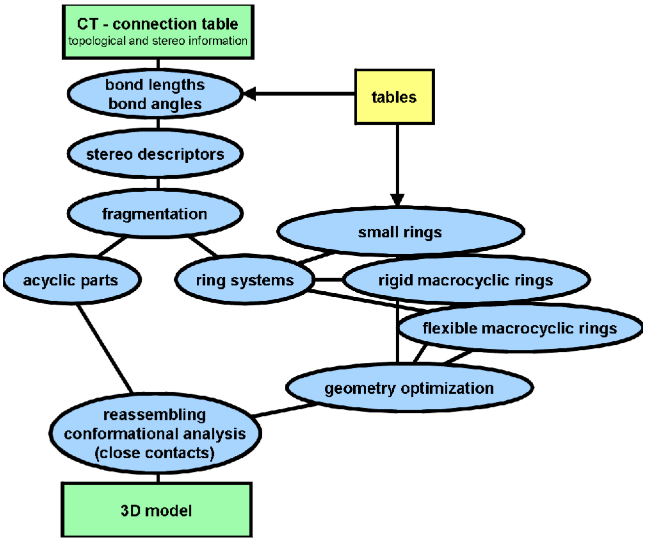

Figure 8 *Outline of the Program Flow in CORINA*

✳ CORINA Version 2.4 is accessible for the free conversion of a maximum of 1,000 structures *via* the Internet: *http://www2.ccc.uni-erlangen.de/software/corina* wide range of applications from infrared spectra simulation [21] to drug design.[22]

Overview on the CORINA algorithm

CORINA is a rule- and data-based program system and can be considered as an automatic model building kit. The generation of 3D molecular models in CORINA is based on a set of rules derived from experimental data and theoretical investigations, such as X-ray crystallography, force field calculations, and geometric considerations. In addition, a condensed set of data on bond lengths, bond angles, and ring geometries is included. The rules and data involved in the build-up process have a broad range of validity to ensure that the program is applicable to a large variety of chemical structures; in fact it covers the entire range of organic chemistry and a large variety of organometallic compounds. Figure 8 shows the general principles of CORINA.

CORINA requires as input a connection table (CT) containing information on the number of atoms, atom types, bonds, and stereochemical descriptors where appropriate. In the first step, bond lengths and bond angles are assigned to standard values depending on atom types, the atomic hybridization states, and the bond order of the atom pair under consideration. Since bond lengths and angles possess only one rigid minimum, these values are taken from a table parameterized for the entire periodic table. For bonds where no appropriate entry can be found in the table, reasonable values are calculated from electronegativity and covalent atomic radii. Atoms with up to six neighbors can be handled according to the Valence Shell Electron Pair Repulsion (VSEPR) model. When stereo-descriptors are lacking, reasonable assumptions are made.

Since torsional angles may assume a series of reasonable values, two major problems arise. First, in ring systems only sets of torsional angles are allowed that fulfill the ring closure condition properly. Secondly, non-bonding interactions between parts of flexible chains must be minimized. Thus, CORINA handles rings and chains separately. A molecule is fragmented into ring systems and acyclic parts. Ring systems are then separated into small rings with up to eight atoms, rigid macrocyclic systems containing large rings with low flexibility and flexible macrocyclic systems consisting of one large flexible ring which might be fused or bridged to small rings.

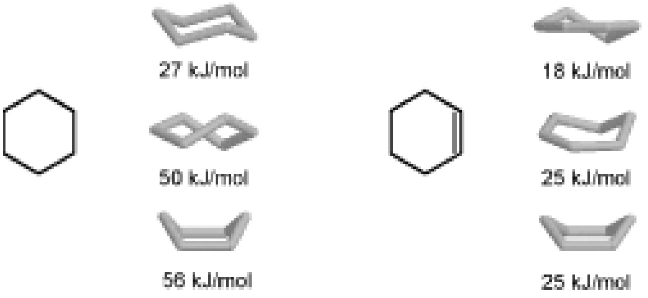

Figure 9 *Ring templates for cyclohexane and cyclohexene*

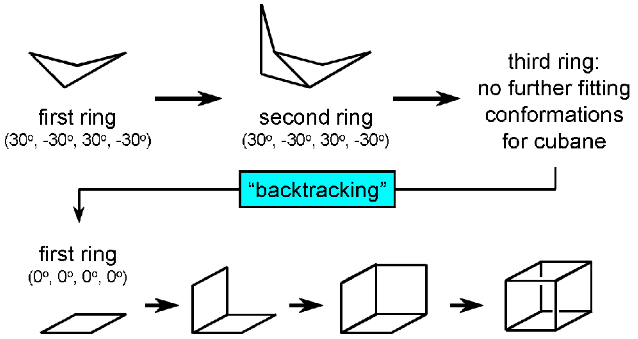

Figure 10 *Backtracking procedure for the generation of a 3D model of cubane*

For small ring systems consisting of less than nine atoms, the number of reasonable conformations is rather limited. Thus, these systems are processed by using a table of allowed single ring conformations. Ring templates are stored as lists of torsional angles, for each ring size and number of unsaturations in the ring, ordered by their conformational energy. Figure 9 gives an example for the conformations of cyclohexane and cyclohexene as they are stored in the ring conformation table.

In the case of fused or bridged systems, a backtracking search procedure finds a contradiction-free set of conformations for each single ring following some geometric and energy restrictions. Figure 10 illustrates this procedure for cubane. After the smallest set of smallest rings (SSSR) has been determined (five four-membered rings in the case of cubane), the algorithm starts with the lowest energy conformation (torsion angle sequence: 30°, -30°, 30°, -30°; envelope form). Two of these conformations can be fit together, but a third one cannot be fused to this assembly. The backtracking procedure then selects the next possible conformation from the list of ring templates (0°, 0°, 0°, 0°, planar

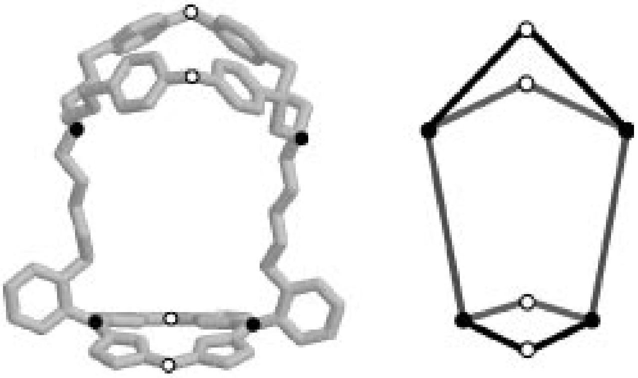

Figure 11 *3D model of a macrocyclic molecule and its corresponding superstructure*

Figure 12 *Superstructures of cyclononane resulting in more than one conformation*

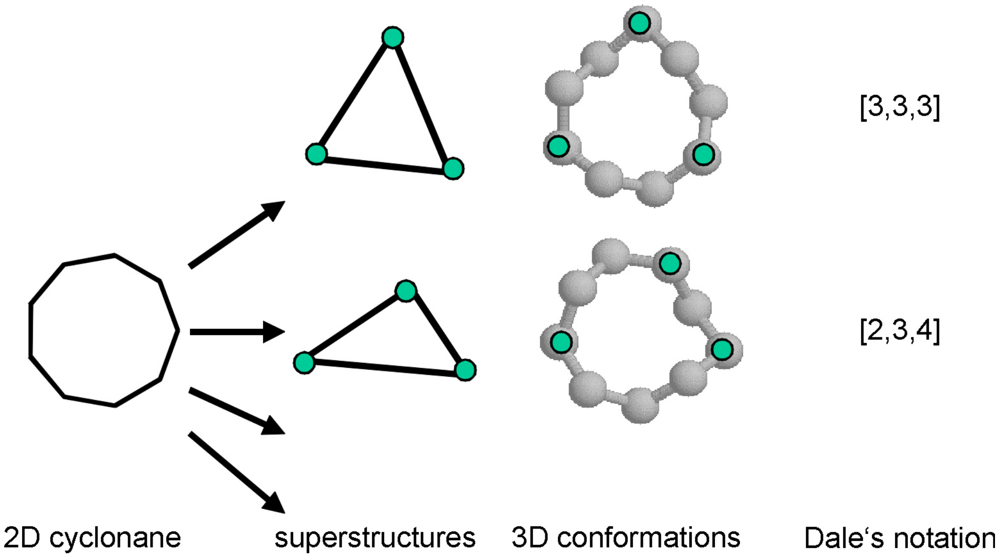

form). Again, the fusion of more than one ring to the envelope form is not possible. Thus, the planar geometry is assigned to the first ring, too, finally leading to the correct skeleton of cubane.

The number of possible conformations rises drastically with increasing ring size. Therefore, large ring systems cannot be handled with the methods applied to small rings. However, in rigid polymacrocyclic structures often an overall general outline can be found, a so-called superstructure. The porphyrin-bridged cyclophane molecule in Figure 11 shows a cage-like superstructure. This superstructure retains approximately the shape and symmetry of the complete system by reducing the original structure to the number of macrocycles and bridgehead atoms (anchor atoms).

The so-called "principle of superstructure" is implemented in CORINA for generating a 3D structure for rigid macrocyclic and polymacrocyclic systems. First, the ring system is reduced to its superstructure, preserving the essential topological features. As this superstructure contains only small rings, albeit with very long bonds, the algorithms described for small ring systems can be applied to generate a 3D model for the superstructure by using long (super-) bonds. Finally, the removed atoms are restored and a complete 3D model of the entire ring system is obtained.

The conformational behavior of flexible macrocyclic structures is quite different. Thus, the method described above cannot be applied to large flexible ring systems, because the definition of one single superstructure is not possible. Figure 12 illustrates this for cyclononane. In such a situation, a conformational analysis procedure generating and evaluating several geometries has been implemented, based on Dale's assumption [23] that large rings exhibit a polygon-like superstructure (Figure 12).[24] This assumption was translated into a 1D representation of the structures, consisting of the numbers of bonds between the corner atoms (anchor atoms of the superstructure) defining the polygon. This linear nota-

Figure 13 *Reduced conformational analysis to avoid non-bonded interactions*

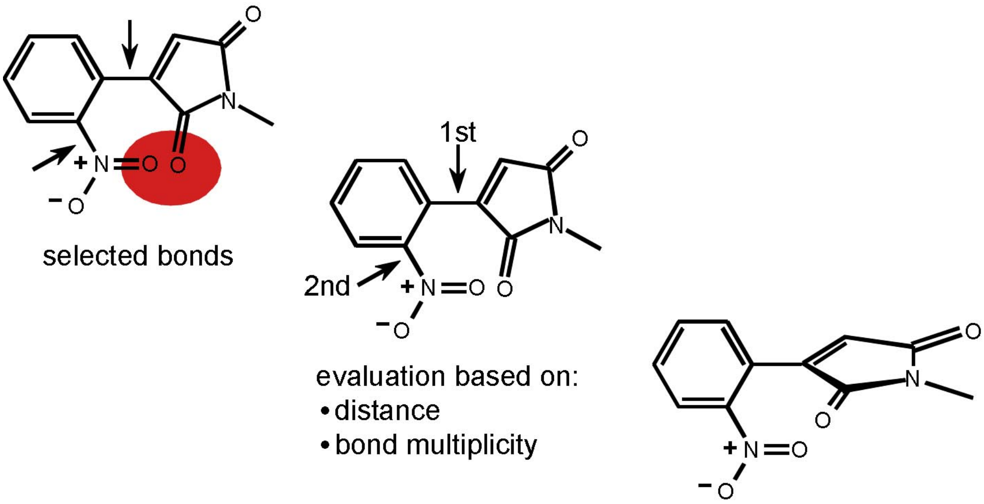

Figure 14 *Histograms of the RMS deviations of the 3D coordinates of the X-ray geometries to those generated with CORINA: All non-hydrogen atoms (***a***); ring atoms only (***b***)*

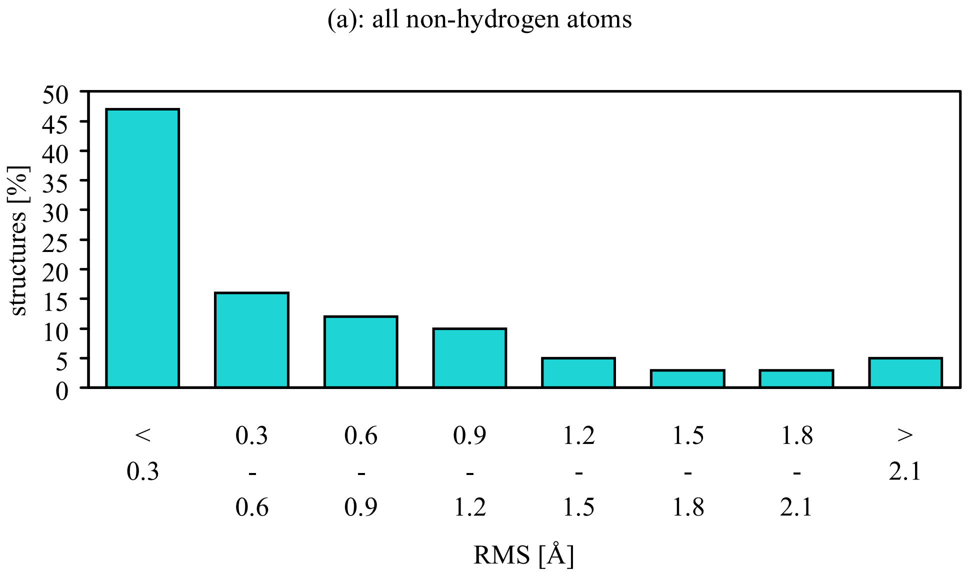

(b): ring atoms only

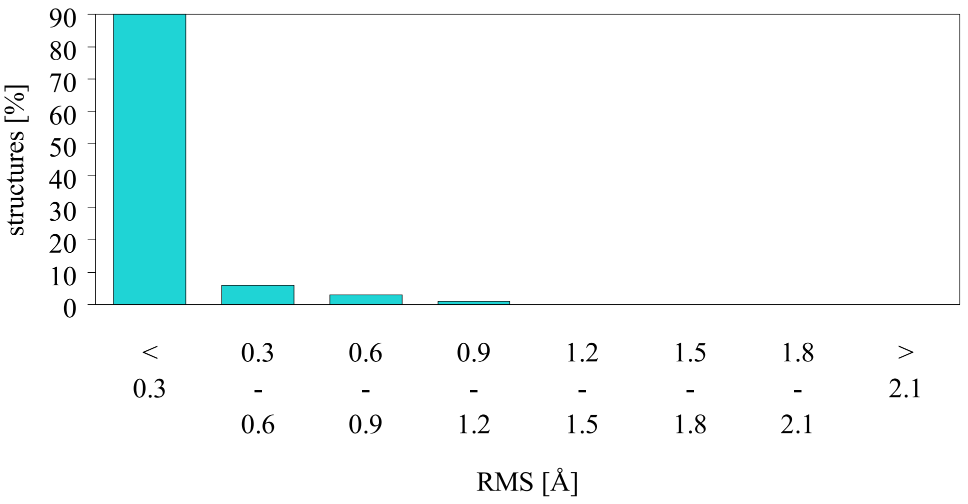

tion can be translated directly into a 3D model and into a symbolic strain energy value for a ranking of the generated conformations.

After generation of the ring systems through the methods described above, CORINA uses a reduced force field to optimize the ring geometries. Two simplifications lead to this so-called pseudo-force field: First, ring systems are considered as rather rigid. Thus, influences of torsional energies and steric influences of exocyclic substituents can be neglected. Only the ring skeletons need to be optimized. Secondly, the major aim is to optimize geometries and not to calculate energies, i.e., no actual energy values need to be calculated. These assumptions result in a large reduction of energy terms to be calculated, guaranteeing a fast convergence after a few iterations and short computation times during the optimization process.

For acyclic fragments and molecules, the principle of longest pathways has been implemented in CORINA. The main chains are stretched as much as possible by setting the torsion angles to *trans* configurations, unless a *cis* double bond is specified. This method effectively minimizes non-bonding interactions.

After combination of the three-dimensional fragments of the ring systems and of the acyclic parts, the complete 3D model is checked for overlap of atoms and for close contacts. If such situations are detected, CORINA performs a reduced conformational analysis to avoid these interactions as follows (Figure 13); firstly, a strategic rotatable bond within the pathway connecting the two interacting atoms is determined, depending on topological features and double bond character. Secondly, the torsional angle of this bond is changed according to rules of conformational preferences of torsional angles in open chain portions derived from a statistical analysis of crystal structures, until non-bonded interactions are eliminated.

Quality of generated molecular models

In order to illustrate the quality of the molecular models generated by CORINA, the program was tested using a dataset of 639 experimentally determined structures from the Cambridge Structural Database (CSD).[25] This test set was compiled by choosing 19 chemical classes from the CSD, each structure containing at least one ring system and a proper stereochemical description. CORINA (version 2.4, December 1998) is able to convert 100% of the structures into 3D within 42 s on a Silicon Graphics R10000 UNIX workstation (0.07 s/molecule). Finally, the models generated were compared to the X-ray structures. Figure 14 shows the histograms of the RMS deviations of the 3D atom coordinates for all non-hydrogen atoms (Figure 14a) and for ring atoms (Figure 14b) of the experimental structures compared to those generated with CORINA. For the comparison of all non-hydrogen atoms, 46% of the structures have an RMS deviation of less than 0.3 Å and can be regarded as identical conformations. Clearly, as open chain structures can exist in a variety of low energy conformations, larger RMS deviations must also be expected. The comparison of ring atoms only shows that CORINA reproduces 90% of the ring geometries almost exactly. A complete study with a previous version of CORINA (version 1.5) including an evaluation of other commercially available model builders is given in [11].

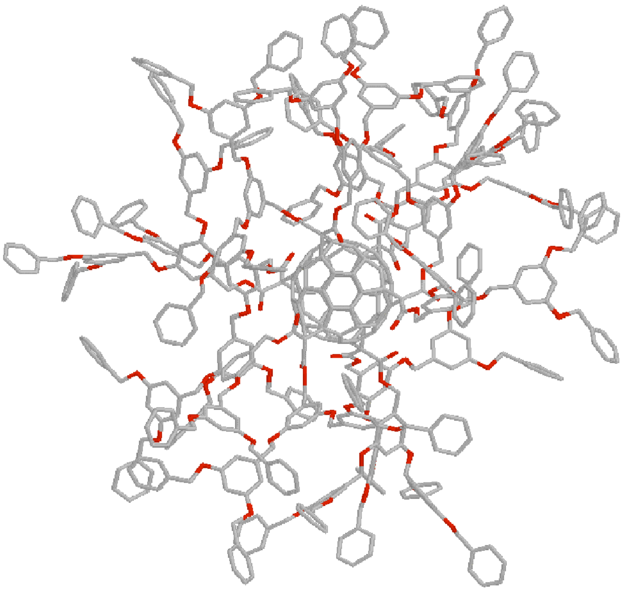

Figure 15 *3D model of the fullerene dendrimer* ***3D*** *consisting of 1278 atoms generated by CORINA*

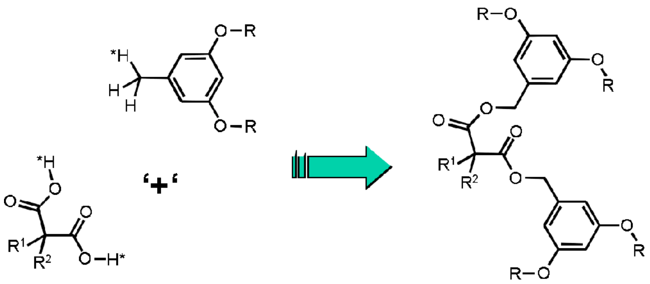

Figure 16 *Automatic combination of molecules to generate a large connection table*

Handling of large datasets

To demonstrate the broad validity of CORINA, the open part of the database of the National Cancer Institute (NCI, Developmental Therapeutics Program) [26] has been converted into 3D molecular models. This dataset contains 246,620 structures and was processed by CORINA (version 2.4) within 18,843 s (0.08 s/molecule) on a Silicon Graphics R10000 UNIX workstation with a conversion rate of 99.5% without program crash or any intervention, a rather impressive performance. 820 compounds were excluded because of structural insufficiencies in the 2D information (e.g. R groups) and only 347 compounds (0.14%) could not be converted by CORINA because of internal problems in the program.

Handling of large molecules: preparation of the input information and modeling of fullerene dendrimeres

Molecular modeling software requires structure information on molecules in machine readable form, in formatted files that can be interpreted by computer programs.

This can be one of the various standard file formats for the handling of chemical data (MDL SDFile, SYBYL MOLFILE, PDB Files, SMILES linear notation, etc.). These structure data files are usually generated automatically by drawing and storing the molecule with the help of graphic molecule editors. The datafiles contain the connection table (CT) of the molecule, consisting of an atom list, a bond table, and stereo descriptors, thus providing the topological features (the constitution) of the structure. This information is sufficient to build up a three-dimensional model of the molecule automatically by CORINA.

Since the molecules in the present investigation are quite large, and the generation of the input data becomes rather time consuming and difficult, there is clearly the need for an automation of this process. Figure 15 shows a fullerene dendrimer, which has been modeled in this study with CORINA, consisting of 1278 atoms (762 non-hydrogen atoms).

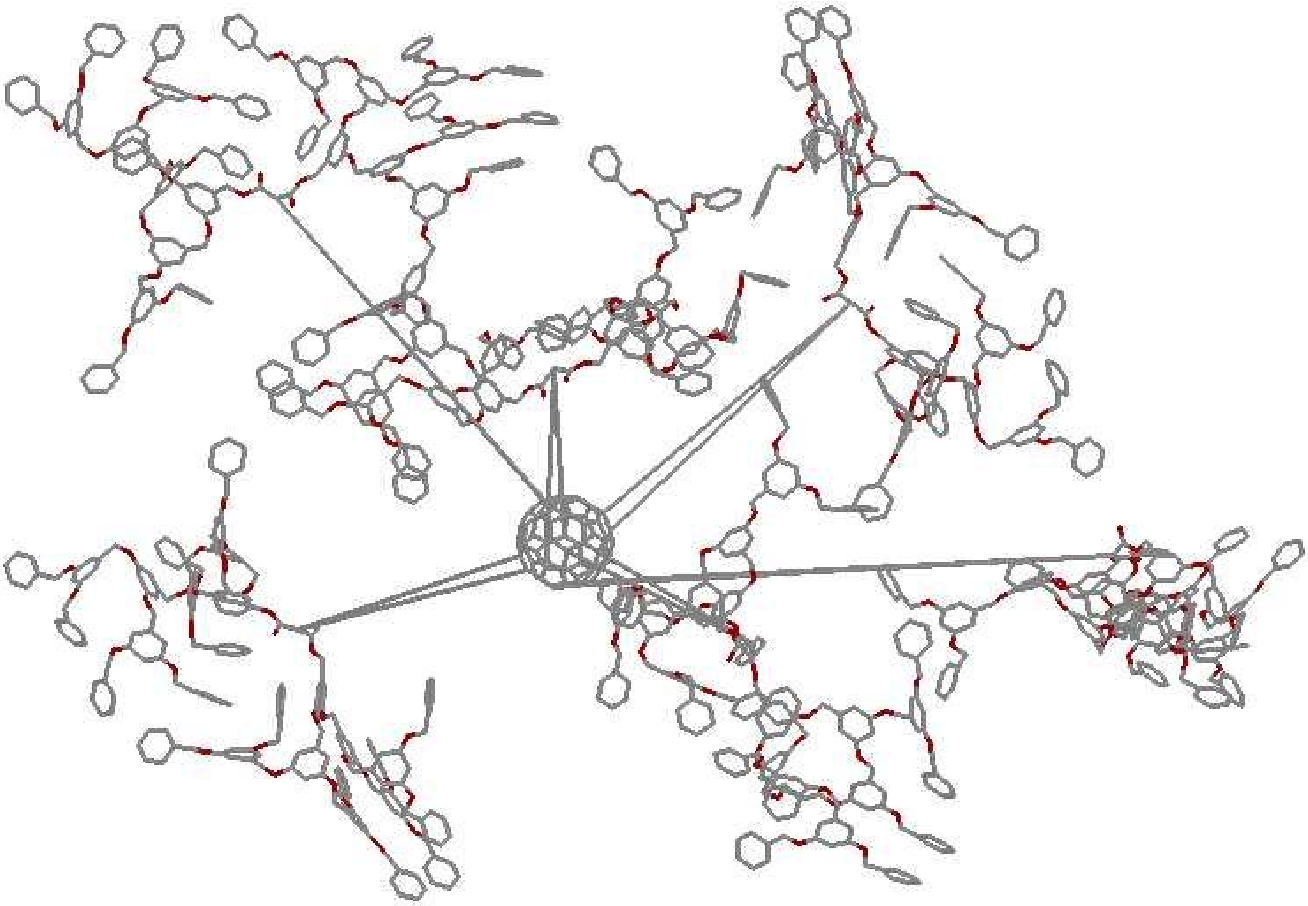

Figure 17 *Starting geometry for MM+ force field optimization*

Thus, a program was developed that automatically generates the CT of the entire molecule by combining smaller and easily accessible building blocks. In the case of highly symmetric structures, like the fullerene dendrimers, this build-up process can be done in a single step. Figure 16 schematically shows the build-up of a dendron in form of a malonic acid derivative with two connection points (marked hydrogen atoms) and a benzyl unit with two ether groups.

The marked hydrogen atoms are eliminated in order to form a new bond between the oxygen atom of the carboxyl group and the exocyclic carbon atom of the toluene derivative. This software tool can also be used for the generation of virtual combinatorial compound libraries by producing all possible combinations of various building blocks.

Experimental section

One of the main problems of this investigation was the generation of a geometry for the compounds under consideration. Due to the high multiplicity of the initiator core with a T_h symmetric hexa-adduct, one rapidly arrives at a sterically overburdened system.

Two approaches were taken: One route generated a rather artificial geometry that was then optimized by force field calculation. The other approach utilized an empirical 3D structure generator that started from information on only the constitution of the molecules concerned.

Starting geometries for MM+ force field calculations

The starting geometry for the force field calculations was built from pre-optimized dendrons, connecting them by methano-bridges with very long bonds of 30-60 Å as shown in Figure 17. This was done to prevent the interruption of the optimization in a local minimum at high energy caused by steric hindrance of the branches. To perform the optimization on such unusual structures, special precautions have to be made as will be explained now.

Force field optimization

The “steepest descent”-optimizer, suitable for investigations of very large systems, cannot be used in this special case as it

Table 1 *Energies (heats of formation) resulting from the different optimization methods. The green columns give the geometries obtained by classical force field optimization (series* ***A****) and of those further processed by simulated annealing (series* ***B****) as well as by molecular dynamics calculations at ambient temperature (series* ***C****). The blue columns show the geometries obtained by CORINA (series* ***D****) and of those further processed by simulated annealing (series* ***E****). Except of the molecules of series* ***C****, all structures have been optimized up to a gradient of 1. All structures can be moved interactively by clicking on the compound name*

	MM+ force field optimization energy [kcal·mol⁻¹]	Molecular dynamics (MM+) 0 K / 1000 K / 0 K 5 ps/15 ps/50 ps energy [kcal·mol⁻¹]	Molecular dynamics (MM+) 300 K 50 ps energy [kcal·mol⁻¹]	CORINA energy [kcal·mol⁻¹]	Molecular dynamics (MM+) 0 K / 1000 K / 0 K 5 ps/15 ps/50 ps energy [kcal·mol⁻¹]
hexa-adducts					
1st generation	766.13	459.02	701.18	593.29	525.74
270 atoms	**1A**	**1B**	**1C**	**1D**	**1E**
2nd generation	1549.09	1471.84	2069.50	720.07	539.60
606 atoms	**2A**	**2B**	**2C**	**2D**	**2E**
3rd generation	1875.50	1526.44	2710.94	1040.90	569.80
1278 atoms	**3A**	**3B**	**3C**	**3D**	**3E**
4th generation	1981.34	964.07	9445.20	4697.08	3657.35
2622 atoms	**4A**	**4B**	**4C**	**4D**	**4E**
mixed hexa-adducts					
2nd generation	1323.59	1274.78	1733.54	666.37	1463.54
534 atoms	**5A**	**5B**	**5C**	**5D**	**5E**
mono-adducts					
4th generation	865.81	578.94	1597.60	788.94	588.02
478 atoms	**6A**	**6B**	**6C**	**6D**	**6E**

rapidly reduces strong forces, i.e., the long bonds are primarily shortened first.

To prevent this, the "Polak-Ribiere"-optimizer with conjugate gradient was applied to distribute the energy of the long bonds onto the branches. Then, all bonds in the system are simultaneously extended and the branches can adjust to the overloaded structure while the long bonds are slowly shortened. The optimization was performed up to a gradient of 0.1.

Molecular dynamics calculations of the pre-optimized structures

Minimum gas phase structures at 0 K Simulated annealing was carried out with the MM+ pre-optimized structures. Starting at 0 K the molecule was heated for 5 ps, equilibrated for 15 ps at 1000 K and cooled to 0 K for 50 ps. Finally, optimization was executed up to a gradient of 0.1.

Gas phase structures at ambient temperature Starting from the same MM+ pre-optimized structure the molecule was equilibrated at "constant temperature" for 50 ps at 300 K.

Semiempirical calculations

The software package SPARTAN used for the calculations was limited to 150 atoms, semiempirical calculation with AM1 was carried out for only one typical case to investigate the π-π-interactions of gas phase structures.

To this end, the structure **7** obtained from simulated annealing was converted into an xyz-file with HyperChem. This file was manually changed to obtain a SPARTAN-type file which was used for a semiempirical single point calculation to obtain information about the electronic behavior of the molecule.

Results

Table 1 summarizes the calculations performed and the results obtained. The structures **1** to **7**, for which the calculations reported in Table 1 were performed are outlined in Table 2. The letters **A**, **B**, **C**, **D**, and **E** refer to different geometries of a compound obtained with the various computational schemes.

Table 2a *Investigated structures*

Structure	Fullerene Core	R_1	R_2
hexa-adducts **1A – 1E** 1st generation 270 atoms	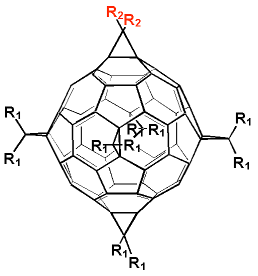	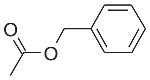	$= R_1$
2A – 2E 2nd generation 606 atoms		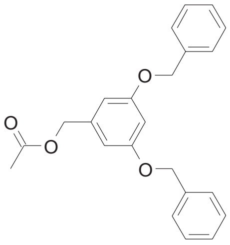	$= R_1$
3A – 3E 3rd generation 1278 atoms		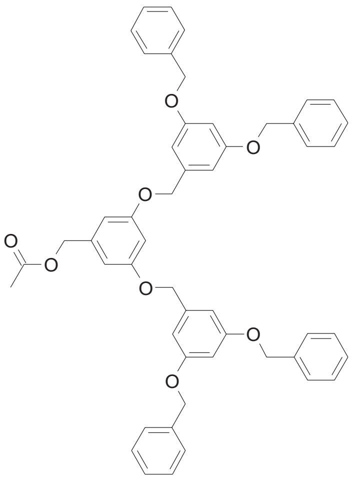	$= R_1$

Table 2b *Investigated structures*

Structure	Fullerene Core	R_1	R_2
hexa-adducts **4A – 4E** 4th generation 2622 atoms		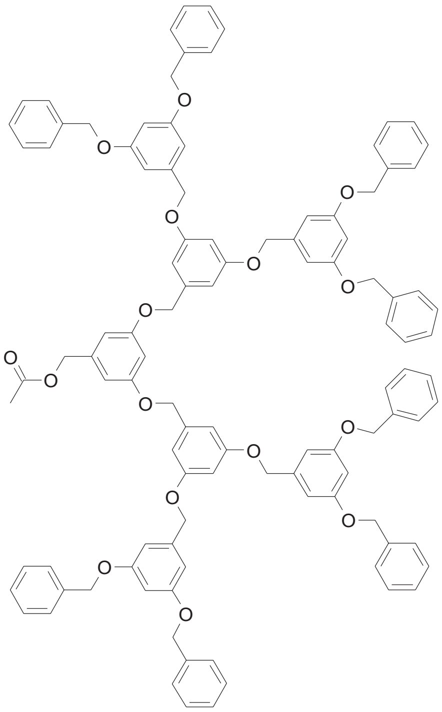	= R_1
mixed hexa-adducts **5A – 5E** 2nd generation 534 atoms	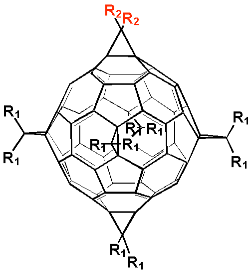	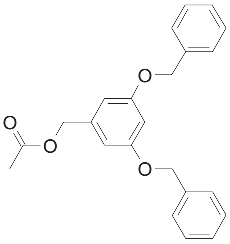	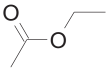

Table 2c *Investigated structures*

Structure	Fullerene Core	R_1	R_2
mono-adducts **6A – 6E** 4th generation 478 atoms	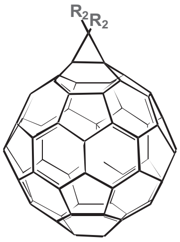		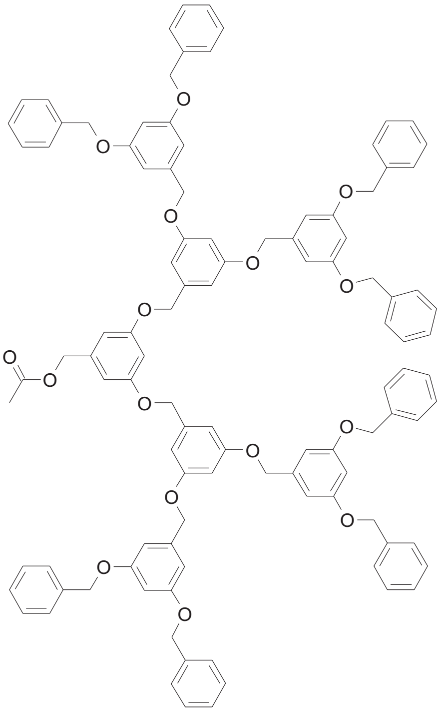
7 1st generation 111 atoms			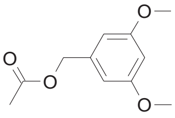

Energies

Some general trends can be observed in the calculations summarized in Table 1.

With three exceptions (**1B**, **4B,** and **6B**), CORINA (series **D**) provides the best geometries (i.e. structures with lowest energies). These energies are even lower than the ones obtained by simulated annealing (series **B**). For the structures **3D** and **4D**, CORINA detects 36 and 1050 close atom contacts, respectively (non-bonded atom distances lower than the sum of the van der Waals radii). This explains the rather high energy values, particularly in the case of **4B**. In these cases, the rules implemented in CORINA are not able to avoid the close contacts. In such situations, CORINA gives a warning message informing about such non-bonded interactions in the structure.

Of course, the energies derived from classical force field optimization (series **A**) are always higher than those obtained after simulated annealing (series **B**). The highest energies originate from molecular dynamics calculations at ambient

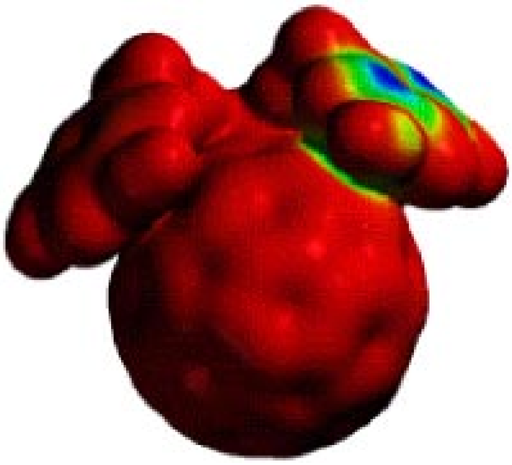

Figure 18 *Projection of the LUMO of **7** onto the electron density surface. The blue areas show a high orbital coefficient, whereas the red areas indicate a low orbital coefficient*

temperature (series **C**) as this is the only method that is not performed at 0 K.

Structures

The following trends can be observed for the geometries of the different molecules.

Series **A**: No systematic characteristics can be derived.

Series **B**: These are all rather compact, globular structures.

Series **C**: The conformations of the dendrimer branches are randomly populated.

Series **D**: Locally symmetric, "crystal-like" structures are obtained with clefts and cavities.

Series **E**: Again, these are all rather compact, globular structures.

Computation times

The molecular mechanics and molecular dynamics calculations were performed on a Pentium system with 200 MHz and 64 MB.

Calculation times range from 3 hours (**6A**) to 71 hours (**4A**) for the classical force field optimizations, from 5 days (**6B**) to 10 weeks (**4B**), or (**4E**) for simulated annealing, and from 4 days (**6C**) to 7 weeks (**4C**) for molecular dynamics calculations at ambient temperature.

The CORINA runs were performed on a Silicon Graphics R10000 Unix workstation with 180 MHz and 256 MB and were much faster, taking only from 2 s (**1D**), 31 s (**2D**), 160 s (**3D**), to 1128 s (**4D**), 24 s (**5D**), and 18 s (**6D**).

Semiempirical calculations

The simulated annealing calculations led to rather compact, globular structures (series **B** and **E**). We therefore performed semiempirical AM1 calculations to investigate whether evidence for an interaction between the fullerene and dendrite can be found within a semiempirical quantum mechanical calculation. A mono-adduct **7** of the first generation of the dendrimer groups was chosen for this investigations.

After simulated annealing of the model compound **7**, a rather compact, globular structure is obtained. A semiempirical single point calculation shows a LUMO shared by

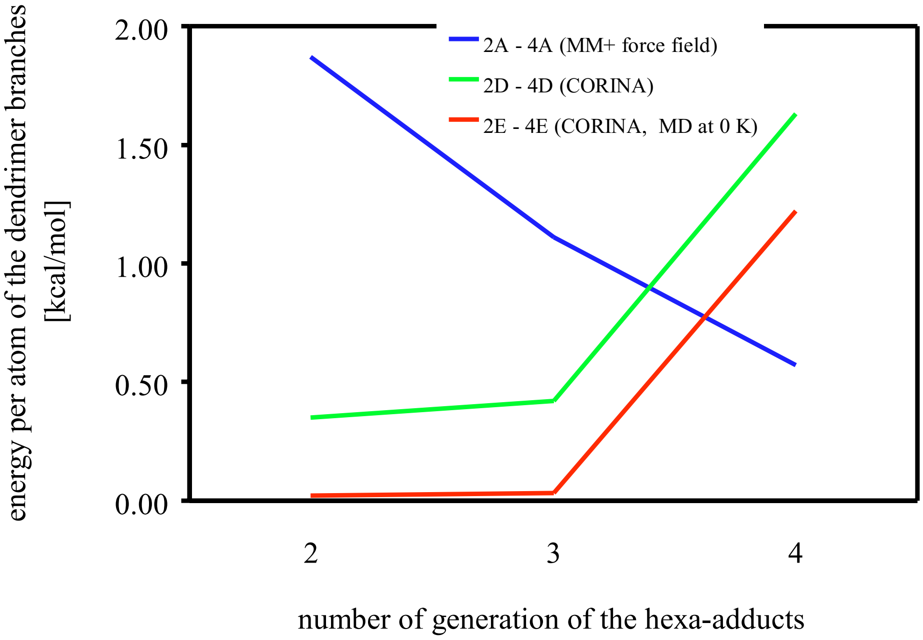

Figure 19 *Energy per atom of the dendrimer branches for the 2nd to 4th generations of the hexa-adducts (**2A** - **4A**, **2D** - **4D**, and **2E** - **4E**)*

both fullerene and the dendrite as illustrated in Figure 18. This indicates π–π-interactions between the fullerene core and the benzene rings of the dendrimer.

Discussion

The analysis of the energies and the geometries of the structures obtained should address a series of questions posed in these investigations.

Energies

Is there a way to distinguish a self-limiting generation for the fullerene-dendrimer-hexa-adducts? A self-limiting generation should be characterized by a rapidly increasing energy. It should be mentioned that the fullerene is an endergonic compound while the branches are exergonic. Thus, to find out a self-limiting generation, the heat of formation of fullerene (527.88 kcal mol^{-1}) is subtracted from the energy of the entire structure and the energy of the dendrimer thus obtained is divided by the number of atoms of the dendrimer.

This method shows (Figure 19) that for the overburdened systems **4**, simulated annealing gives lower energies than CORINA. This is also the case when globular structures can be formed through π–π-interactions (**6B**).

The heats of formation obtained by simulated annealing at ambient temperature (series **C**) can not be compared to the energies at 0 K of the series **A**, **D**, and **E**. The compounds of series **C** have been equilibrated at 300 K for the investigation on cavities or clefts within the structure at room temperature.

Structures

Are the structures from simulated annealing "realistic"? As shown in semiempirical calculations (**7**), π–π-interactions provide the compact structures, thus verifying the results from simulated annealing. These geometries should therefore be realistic models for the structures in the gas phase at 0 K.

Are the structures from CORINA "realistic"? Because of the methods implemented in the structure generation algorithm of CORINA, the geometries obtained are more "crystal-like", forming clefts and cavities.

For very large, sterically overloaded systems where one would need a careful geometry-fitting procedure to find a feasible 3D structure, the rule- and data-based method reaches its limits.

As CORINA is based on knowledge derived from experimental data (e.g. X-ray crystal structures) obtained at room temperature, the geometries generated by this method should differ from structures at 0 K in the gas phase. However, CORINA provides a simple and rapid access to good starting geometries for molecular dynamics and simulated annealing calculations.

Which structures can be expected at room temperature? To obtain a picture of the structures at ambient temperature, an equilibration at 300 K (series **C**) was performed instead of an optimization at 0 K. The molecule **5C** was taken as a model compound for dendrizymes, as it was expected to develop cavities.

Video Clip 1 shows the trajectory of the molecular dynamics calculations of compound **5C** at 300 K. The pink regions show the fullerene core, the blue parts indicate the dendrimer branches, and the yellow areas the ethylester groups. The dendrimer branches of **5C** are quite flexible. There is free access to the yellow parts of the molecule (ethylester groups). This indicates that no cavity should be formed around an active site at the second generation of the dendrimer.

How can minimum structures be found for sterically overburdened systems? With highly complex molecules, classical force field optimization (series **A**) and CORINA (series **D**) might get stuck in local minima at high energies. In such situations, molecular dynamics is the best method to arrive at minimum structures for such large systems. During the simulated annealing all bonds are extended, enabling the branches to rotate in any direction. Thus, they can fit to an ideal conformation in the cooling process.

This is demonstrated in Video Clip 2 for the compound **5B**. It shows the trajectory of the molecular dynamics calculations of compound **5B** at 1000 K and then cooling to 0 K. The pink regions show the fullerene core, the blue parts indicate the dendrimer branches, and the yellow areas the ethylester groups.

To give an insight into the flexibility of large systems at high temperatures, the trajectory of the molecular dynamics calculations of compound **4B**, the largest system modeled in

---

Video Clip 1 *Trajectory of the molecular dynamics calculations of compound* ***5C*** *at 300 K. (By clicking on this legend, a video clip is started showing the behavior of compound 5C at 300 K. The pink regions show the fullerene core, the blue parts indicate the dendrimer branches and the yellow areas the ethylester groups)*

Video Clip 2 *Trajectory of the molecular dynamics calculations of compound* ***5B*** *at 1000 K and cooling to 0 K. (By clicking on this legend, a video clip is started showing the behavior of compound 5B at 1000 K and then cooling to 0 K. The pink regions show the fullerene core, the blue parts indicate the dendrimer branches and the yellow areas the ethylester groups)*

Video Clip 3 *Trajectory of the molecular dynamics calculations of compound* ***4B*** *at 1000 K and then cooling to 0 K. (By clicking on this legend, a video clip is started showing the behavior of compound 4B at 1000 K and then cooling to 0 K. The pink regions show the fullerene core and the blue parts indicate the dendrimer branches)* this study, at 1000 K is shown in Video Clip 3. The pink regions show the fullerene core, the blue parts indicate the dendrimer branches.

Conclusions

One major aim of this study was to develop computational methods able to predict and to model three-dimensional structures for very large molecular systems, such as the fullerene dendrimers described. Two approaches have been developed and used successfully to solve this problem: Classical force field calculations for structure optimization and molecular dynamics calculations and the rule- and data-based 3D model builder CORINA.

In most cases, structures with the lowest energies were obtained by the structure generator CORINA. This is the more gratifying, as CORINA has fast and simple building procedures compared to the rather time-consuming construction methods of the MM+ force field. Starting with the CORINA geometries, post-processing by simulated annealing leads to the lowest energies obtained during this study. The computation times of the CORINA runs are orders of magnitude shorter than those of the other methods. On the other hand, the algorithm implemented in CORINA reaches its technical limits at sterically overburdened systems like the fullerene hexa-adducts with the fourth generation of dendrimers (series **4** with 2622 atoms but 1050 close atom contacts). Nevertheless, CORINA is able to give a fast and reliable insight into the three-dimensional world of very complex and large systems.

The question where a self-limiting generation of the fullerene dendrimers is obtained cannot be answered completely within this study. The heats of formation of the fourth generation (series **4**) show that there might be space for at least one additional generation. The computations necessary for clarifying this question within reasonable computation times would require large and powerful supercomputers.

Simulated annealing and the calculated trajectories of the fullerene mixed hexa-adduct dendrimers (series **5**) show a relatively free accessible non-dendrimer substituted conjunction point of the fullerene, i.e., there is no evidence for cavities within the structure to form “dendritic boxes” or host-guest-complexes.

The compact and globular structures obtained from molecular dynamics calculations are mirrored by the results of semiempirical quantum mechanical calculations (**7**). These show π–π-interactions between the fullerene core and the benzyl groups of the dendrimer branches.

Acknowledgements We gratefully acknowledge inspiring discussions with Dr. Jens Sadowski (BASF AG) and want to thank him for his work on the development of the 3D structure generator CORINA. We also thank the Bundesministerium für Bildung und Forschung for financial assistance.

Supplementary material available The structures (**1A–1E**, **2A–2E**, **3A–3E**, **4A–4E**, **5A–5E**, and **6A–6E**) which have been modeled in this study are available in PDB file format for download in Table 1. The trajectories of the molecular dynamics calculations of the structures **4B**, **5B**, and **5C** (Video Clips 1-3) are available for download in mpeg file format.

References

1. Buhleier, E.; Wehner, W.; Vögtle, F. *Synthesis* **1978**, 155.
2. Newcome, G. R.; Lin, X.-F. *Macromolecules* **1991**, *24*, 1443.
3. Wooley, K. L.; Hawker, C. J.; Fréchet, J. M. *J. Chem. Soc., Perkin Trans. 1* **1991**, *1*, 1059.
4. Tomalia, D. A.; Naylor, A. M.; Goddard III, W. A. *Angew. Chem.* **1990**, *102*, 132.
5. De Gennes, P. G.; Hervet, H. *J. Physiques-Lettres* **1983**, *44*, L-351.
6. Newcome, G. R.; Nayak, A.; Behera, R. K.; Moorefield, C. N.; Baker, G. R. *J. Org. Chem.* **1992,** *57*, 358.
7. Jansen, J. F. G. A.; de Brabander-van den Berg, E. M. M.; Meijer, E. W. *Science* **1994**, *266*, 1266.
8. Camps, X.; Schönberger, H.; Hirsch, A. *Chem. Eur. J.* **1997**, *3*, 561.
9. Schönberger, H., Diploma Thesis, Friedrich-Alexander-Universität Erlangen-Nürnberg, 1996 (*http://www2.ccc.uni-erlangen.de/dissertationen/data/diplom/Hubert_Schoenberger/html*).
10. HyperChem, Version 4.5, Hypercube, Inc.: Gainesville, FL, USA, 1994.
11. Sadowski, J.; Gasteiger, J.; Klebe, G. *J. Chem. Inf. Comput. Sci.* **1994**, *34*, 1000.
12. Camps, X.; Dietel, E.; Hirsch, A.; Pyo, S.; Echegoyen, L.; Hackbarth, S.; Roeder, B. *Chem. Eur. J.* **1999**, *5*, in press.
13. Djojo, F.; Hirsch, A. *Chem. Eur. J.* **1998**, *2*, 344.
14. SPARTAN, Version 4.0; Wavefunction, Inc.: Irvine, CA, USA, 1995.
15. Hiller, C.; Gasteiger, J. In *Software-Entwicklung in der Chemie*; Gasteiger, J., Ed.; Springer: Berlin, 1987; Vol 1, pp 53-66.
16. Sadowski, J.; Gasteiger, J. *Chem. Rev.* **1993**, *93*, 2567.
17. Gasteiger, J.; Rudolph, C.; Sadowski, J. *Tetrahedron Comput. Methodol.* **1990**, *3*, 537.
18. CORINA, Version 2.4, Molecular Networks GmbH: Erlangen, Germany, 1999 (*http://www.mol-net.de*).
19. Gasteiger, J.; Hutchings, M. G.; Christoph, B.; Gann, L.; Hiller, C.; Löw, P.; Marsili, M.; Saller, H.; Yuki, K. *Top. Curr. Chem.* **1987**, *137*, 19.
20. Gasteiger, J.; Ihlenfeldt, W. D.; Röse, P. *Recl. Trav. Chim. Pays-Bas* **1992**, *111*, 270.
21. Schuur, J. H.; Selzer, P.; Gasteiger, J. *J. Chem. Inf. Comput. Sci.* **1996**, *36*, 334.
22. Handschuh, S.; Wagener, M.; Gasteiger, J. *J. Chem. Inf. Comput. Sci.* **1998**, *38*, 220.
23. Dale, J. *Acta Chem. Scand.* **1973**, *27*, 1115.

24. Sadowski, J.; Gasteiger, J. In *Software Development in Chemistry*; Ziessow, D., Ed.; Gesellschaft Deutscher Chemiker: Frankfurt (Main), 1993; Vol 7, pp 65-76.
25. Cambridge Structural Database: Allen, F. H.; Bellard, S.; Brice, M. D.; Cartwright, B. A.; Doubleday, A.; Higgs, H.; Hummelink, T.; Hummelink-Peters, B. G.; Kennard, O.; Motherwell, W. D. S.; Rodgers, J. R.; Watson, D. G. *Acta Crystallogr., Sect. B* **1979**, *35*, 2331.
26. National Cancer Institute, National Institute of Health: Developmental Therapeutics Program, *DTP / 2D and 3D Structural Information*, http://dtp.nci.nih.gov/docs/3d_database/structural_information/structural_data.html.